

Trilateration Localization for Multi-Robot Teams

Paul M. Maxim¹, Suranga Hettiarachchi², William M. Spears¹, Diana F. Spears¹,
Jerry Hamann¹, Thomas Kunkel¹, and Caleb Speiser¹

¹ University of Wyoming, Laramie, Wyoming 82070, USA
{paulmax, wspears, dspears, hamann, caleb485}@uwyo.edu
<http://www.cs.uwyo.edu/~wspears>

² Eastern Oregon University, La Grande, Oregon 97850, USA
suranga.hettiarachchi@eu.edu

Abstract. The ability of robots to quickly and accurately localize their neighbors is extremely important for robotic teams. Prior approaches typically rely either on global information provided by GPS, beacons and landmarks, or on complex local information provided by vision systems. In this paper we describe our trilateration approach to multi-robot localization, which is fully distributed, inexpensive, and scalable [15]. Our prior research [14] focused on maintaining multi-robot formations indoors using trilateration. This paper pushes the limits of our trilateration technology by testing formations of robots in an outdoor setting at larger inter-robot distances and higher speeds.

1 Introduction

The main contributions of this paper are: (1) a presentation of our trilateration approach to multi-robot localization (i.e., each robot locates its neighbors), and (2) a set of experimental results obtained with our trilateration approach under outdoor conditions. These experimental results highlight the advantages of our approach and clarify its limitations. The outdoor experiments are conducted in an environment with varying terrain (e.g., grass, dirt, and concrete), rocks, protruding tree roots, leaves, pine cones and other ground protrusions. Also, there was a considerable amount of dust and wind (over 9 meters per second). Despite this, the robots are able to maintain high quality formations.

The organization of this paper is as follows. Section 2 introduces our trilateration approach to localization, which is fully distributed and assumes that each robot has its own local coordinate frame (i.e., no global information is required). Each robot determines its neighbors' range and bearing with respect to its own egocentric, local coordinate system. After such localization, sensor values and other data can be exchanged between robots in a straightforward manner. Next, sections 3, 4 and 5 describe our trilateration implementation and current robot platforms. Sections 6 and 7 present results from our experiments. Section 8 summarizes and concludes the paper.

2 Localization via Trilateration

The purpose of our trilateration technology is to create a plug-in hardware module to accurately localize neighboring robots, without global information and/or the use of vision

systems. Our localization technology does not preclude the use of other technologies. Beacons, landmarks, vision systems, GPS [6], and pheromones are not necessary, but they can be added if desired. It is important to note that our trilateration approach is not restricted to one particular class of control algorithms – it is useful for behavior-based approaches [1], control-theoretic approaches [2, 3], motor schema algorithms [4], and physicomimetics [5, 16, 17].

In 2D *trilateration*, the locations of three base points are known as well as the distances from each of these three base points to the object to be localized. Looked at visually, 2D trilateration involves finding the location where three circles intersect. Thus, to locate a robot using 2D trilateration the sensing robot must know the locations of three points in its own coordinate system and be able to measure distances from these three points to the sensed robot.

2.1 Measuring Distance

Our distance measurement method exploits the fact that sound travels significantly more slowly than light, thereby enabling us to employ a Difference in Time of Arrival technique. To tie this to 2D trilateration, assume that each robot has one radio frequency (RF) transceiver and three ultrasonic acoustic transducers. The ultrasonic transducers are the “base points.” Suppose robot 2 simultaneously emits an RF pulse and an ultrasonic acoustic pulse. When robot 1 receives the RF pulse (almost instantaneously), a clock on robot 1 starts. When the acoustic pulse is received by each of the three ultrasonic transducers on robot 1, the elapsed times are computed. These three times are converted to distances, according to the speed of sound. Because the locations of the acoustic transducers are known, robot 1 is now able to use trilateration to compute the location of robot 2 (precisely, the location of the emitting acoustic transducer on robot 2). Of the three acoustic transducers, all three must be capable of receiving, but only one must be capable of transmitting.

Measuring the elapsed times is not difficult. Since the speed of sound is roughly 340.2 meters per second at standard temperature and pressure, it takes approximately 2.9 ms for sound to travel one meter. Times of this magnitude are easily measured using inexpensive electronic hardware.

2.2 Channeling Acoustic Energy into a Plane

Ultrasonic acoustic transducers produce a cone of energy along a line perpendicular to the surface of the transducer. The width of this main lobe (for the inexpensive 40 kHz transducers used in our implementation) is roughly 30° . To produce acoustic energy in a 2D plane would require 12 acoustic transducers in a ring. To get three base points would hence require 36 transducers. This is expensive and is a large power drain. We adopted an alternative approach. Each base point is comprised of one acoustic transducer pointing downward. A parabolic cone [15] is positioned under the transducer, with its tip pointing up toward the transducer (see Figure 2 later in this paper). The parabolic cone acts like a lens. When the transducer is placed at the virtual “focal point” the cone “collects” acoustic energy in the horizontal plane, and focuses this energy to the receiving

acoustic transducer. Similarly, a cone also functions in the reverse, reflecting transmitted acoustic energy into the horizontal plane. This works extremely well – the acoustic energy is detectable to a distance of 3.5 m. which is adequate for our needs. Greater range can be obtained with more power (the scaling appears to be quite manageable).

2.3 Related Work

Trilateration is a well-known technique for robot localization. Most approaches (including ours) are algebraic, although recently a geometric method was proposed [7]. Many localization techniques, including those involving trilateration, use global coordinates [8]; however ours relies on local coordinates only.

MacArthur [9] presents two different trilateration systems. The first uses three acoustic transducers, but without RF. Localization is based on the differences between distances rather than the distances themselves. The three acoustic transducers are arranged in a line. The second uses two acoustic transducers and RF in a method similar to our own. Unfortunately, both systems can only localize points “in front” of the line.

Cricket [10] is another system that makes use of RF and ultrasound for localization. It was developed to be used indoors. Compared to our system, which does not require fixed beacons, the Cricket requires beacons attached to fixed locations in order to function. This is not practical for mobile robot localization in outdoor environments.

Our particular approach was inspired by the CMU *Millibot* project. They also use RF and acoustic transducers for trilateration. However, due to size limitations, each Millibot has only one acoustic transducer (coupled with a right-angle cone, rather than the parabolic cone we use). Hence trilateration is a collaborative endeavor that involves several robots. To perform trilateration, a minimum of three Millibots must be stationary and serve as beacons at any moment in time. The set of three stationary robots changes as the robot team moves. The minimum team size is four robots (and is preferably five). Initialization generally involves having some robots make L-shaped maneuvers, in order to disambiguate the localization [11]. Our approach operates with as few as two robots (but is scalable to an arbitrary number), due to the presence of three acoustic transducers on each robot (see below).

In terms of functionality, an alternative localization method in robotics is to use line-of-sight infra-red (IR) transceivers. When IR is received, signal strength provides an estimate of distance. The IR signal can also be modulated to provide communication. Multiple IR sensors can be used to provide the bearing to the transmitting robot (e.g., see [12, 13]). We view this method as complementary to our own; however, our method is more appropriate for tasks where greater localization accuracy is required. This is especially important in outdoor situations where water vapor or dust could change the IR opacity of air. Similar issues arise with the use of cameras and omni-directional mirrors/lenses, which require far more computational power and a light source.

3 Our Trilateration Approach

Our trilateration approach to localization is illustrated in Figure 1. Assume two robots, shown as circles. An RF transceiver is in the center of each robot. Each robot has three

acoustic transducers (also called *base points*), labeled **A**, **B**, and **C**. Note that the robot's local XY coordinate system is aligned with the L-shaped configuration of the three acoustic transducers, as shown in the figure. *Note, Y points to the front of the robot.*

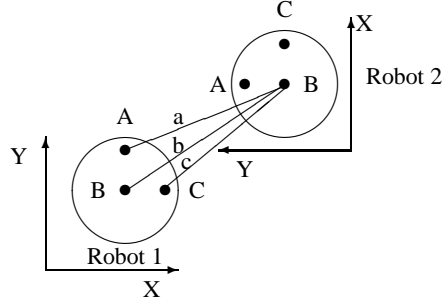


Fig. 1. Three base points in an XY coordinate system pattern.

In Figure 1, robot 2 simultaneously emits an RF pulse and an acoustic pulse from its transducer **B**. Robot 1 then measures the distances **a**, **b**, and **c**. Without loss of generality, assume that transceiver **B** of robot 1 is located at $(x_{1B}, y_{1B}) = (0, 0)$ [15].³ In other words, let **A** be at $(0, d)$, **B** be at $(0, 0)$, and **C** be at $(d, 0)$, where d is the distance between **A** and **B**, and between **B** and **C** (see Figure 1).

For robot 1 to determine the position of **B** on robot 2 within its own coordinate system, it needs to find the simultaneous solution of three nonlinear equations, the intersecting circles with centers located at **A**, **B** and **C** on robot 1 and respective radii of **a**, **b**, and **c**:

$$(x_{2B} - x_{1A})^2 + (y_{2B} - y_{1A})^2 = a^2 \quad (1)$$

$$(x_{2B} - x_{1B})^2 + (y_{2B} - y_{1B})^2 = b^2 \quad (2)$$

$$(x_{2B} - x_{1C})^2 + (y_{2B} - y_{1C})^2 = c^2 \quad (3)$$

Given the transducer configuration shown above, we get [15]:

$$x_{2B} = \frac{b^2 - c^2 + d^2}{2d} \quad y_{2B} = \frac{b^2 - a^2 + d^2}{2d}$$

An interesting benefit of these equations is that they can be simplified even further, if one wants to trilaterate purely in hardware [14].

By allowing robots to share coordinate systems, robots can communicate their information arbitrarily far throughout a robotic network. For example, suppose robot 2 can localize robot 3. Robot 1 can localize only robot 2. If robot 2 can also localize robot 1 (a fair assumption), then by passing this information to robot 1, robot 1 can

³ Subscripts denote the robot number and the acoustic transducer. The transducer **A** on robot 1 is located at (x_{1A}, y_{1A}) .

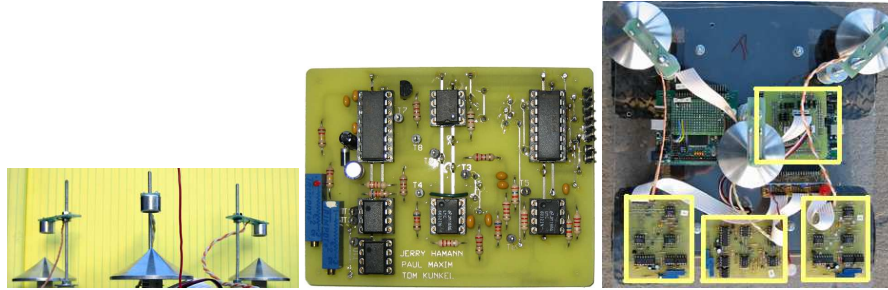


Fig. 2. The acoustic transducers and parabolic cones (left). The XSRF acoustic sensor printed circuit board (middle), and the completed trilateration module (top-down view, right).

now determine the position of robot 3. Furthermore, robot orientations can also be determined. Naturally, localization errors can compound as the path through the network increases in length, but multiple paths can be used to alleviate this problem to some degree. Heil [15] provides details on these issues.

In addition to localization, our trilateration system can also be used for data exchange. Instead of emitting an RF pulse that contains no information but only performs synchronization, we can also append data to the RF pulse. Simple coordinate transformations allow robot 1 to convert the data from robot 2 (which is in the coordinate frame of robot 2) to its own coordinate frame.

4 Trilateration Implementation

Figure 2 illustrate how our trilateration framework is currently implemented in hardware. Figure 2 (left) shows three acoustic transducers pointing down, with reflective parabolic cones. The acoustic transducers transmit and receive 40 kHz acoustic signals.

Figure 2 (middle) shows our in-house acoustic sensor boards (denoted as “XSRF” boards, for *Experimental Sonic Range Finder*). There is one XSRF board for each acoustic transducer. The XSRF board calculates the time difference between receiving the RF signal and the acoustic pulse. Each XSRF contains 7 integrated circuit chips. A MAX362 chip controls whether the board is in transmit or receive mode. When transmitting, a Microchip PIC microprocessor generates a 40 kHz signal. This signal is sent to an amplifier, which then interfaces with the acoustic transducer. This generates the acoustic signal.

In receive mode, a trigger indicates that an RF signal has been heard and that an acoustic signal is arriving. When the RF is received, the XSRF board starts counting. To enhance the sensitivity of the XSRF board, three stages of amplification occur. Each of the three stages is accomplished with a LMC6032 operational amplifier, providing a gain of roughly 15 at each stage. Between the second and third stage there is a 40 kHz bandpass filter to eliminate out-of-bound noise that can lead to saturation. The signal is then passed to two comparators, set at thresholds of ± 2 VDC. When the acoustic energy

exceeds either threshold, the XSRF board finishes counting, indicating the arrival of the acoustic signal.

The timing counts provided by each of the XSRF boards is sent to a MiniDRAGON⁴ powered by a Freescale 68HCS12 microprocessor that performs the trilateration calculations. Figure 2 (right) shows the completed trilateration module from above. The MiniDRAGON is outlined near the center and the three XSRF boards are outlined at the bottom.

4.1 Synchronization Protocol

Trilateration involves at least two robots. One transmits the acoustic-RF pulse combination, while the others use these pulses to compute (trilaterate) the coordinates of the transmitting robot. Hence, trilateration is a one-to-many protocol, allowing multiple robots to simultaneously trilaterate and determine the position of the transmitting robot. Our “token passing” scheme to allow robots to take turns transmitting is not used for the experiments in this paper, to simplify the experimental design. Only leader/follower experiments are presented herein.

5 Maxelbot Platforms

Our University of Wyoming “Maxelbot” (named after the two graduate students who designed and built the robot) is modular. The platform is an MMP5, made by The Machine Lab⁵. Figure 3 (left) shows four Maxelbots. A primary MiniDRAGON is used for control. It communicates via an I²C bus to all other peripherals, allowing us to plug in new peripherals as needed. Figure 3 (right) shows the architecture. The primary MiniDRAGON is the board that drives the motors. It also monitors proximity sensors and shaft encoders. The trilateration module is shown at the top of the diagram. This module controls the RF and acoustic components of trilateration. Additional modules have been built for digital compasses, thermometers, and chemical plume tracing [14]. The PIC processors provide communication with the I²C bus.

6 Trilateration Accuracy as a Function of Velocity and Distance

In [14] we presented the accuracy of our trilateration technique on stationary robots, to a distance of one meter. In this paper we present results for a moving Maxelbot on a treadmill from 0.5 to 3.5 meters behind a stationary Maxelbot placed ahead of the treadmill, at two speeds: 0.32 m/s and 0.64 m/s. Hence we are measuring the accuracy of the performance of the whole system, including the trilateration module and our physicomimetics control algorithm. The results shown are the mean \pm range of the *error* \equiv *ideal_distance* - *measured_distance* (in cm), as measured physically with a ruler (see Tables 2 and 1). Above 3.5 m the acoustic signal is lost, because the acoustic energy falls below the threshold of ± 2 VDC and hence is not detected.

⁴ Produced by Wytec (<http://www.evbplus.com/>)

⁵ See <http://www.themachinelab.com/MMP-5.html>

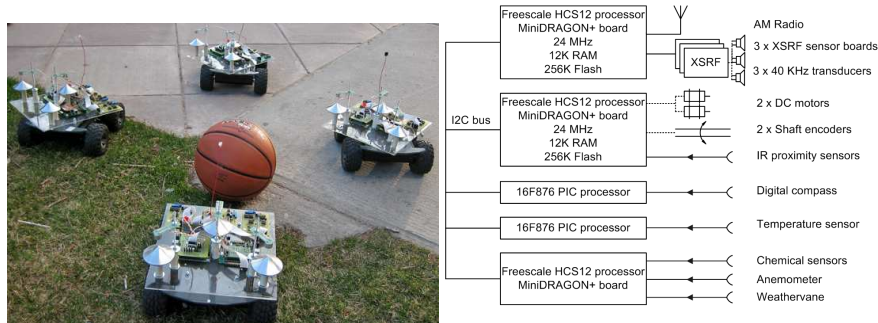


Fig. 3. Maxelbots and the architecture.

The mean error in X is very small ($< 1\%$), which means that the side-to-side position of the Maxelbot is very close to the desired position. The mean error in Y is larger, and at higher distances the Maxelbot lags more behind the desired position (but the mean error is $< 5\%$). However, note that the range in error is less at the higher velocity. The increased momentum of the robot helps filter sensor noise.

Table 1. Mean and range of error of the followers' X position at different distances and velocities.

Velocity	Ideal Distance (cm)						
	50	100	150	200	250	300	350
0.32 m/s	0.0 ± 0.2	0.3 ± 0.3	-0.3 ± 0.3	-0.6 ± 0.4	0.6 ± 0.5	1.9 ± 0.6	0.6 ± 0.6
0.64 m/s	0.0 ± 0.6	0.3 ± 0.3	-1.3 ± 0.9	-1.0 ± 1.0	1.0 ± 1.0	1.9 ± 1.1	0.0 ± 1.3

Table 2. Mean and range of error of the followers' Y position at different distances and velocities.

Velocity	Ideal Distance (cm)						
	50	100	150	200	250	300	350
0.32 m/s	-1.0 ± 1.6	0.0 ± 1.3	-1.3 ± 2.5	-1.9 ± 3.2	-1.3 ± 5.1	-5.0 ± 10.2	-5.0 ± 7.6
0.64 m/s	-5.7 ± 0.6	-0.6 ± 1.9	-3.8 ± 2.5	-5.1 ± 3.8	-3.2 ± 4.4	-14.0 ± 3.8	-16.5 ± 3.8

7 Outdoor Experiments

This section presents three experiments that test the trilateration system outside. In particular, the Maxelbots are run in a region in the center of the University of Wyoming

campus. This region consists mostly of grass, of average height 5 cm, interspersed with concrete sidewalks, trees, rocks, leaves, and other debris. The grass hits the bottom of the Maxelbot. Although generally flat, the ground slope can change rapidly (within 0.6 m), by up to 20°, at boundaries. Results presented below are averaged over five independent runs, each taken over a 20 minute interval. The speed of the robots is approximately 0.55 m/s. For these experiments we are forced to use the trilateration readings themselves as an estimate to the quality of the formation. Given the accuracy of the results in the prior section, this is a reasonable and practical approach.

7.1 Accuracy of a Linear Formation

The first experiment has three Maxelbots in a linear formation. The purpose of this experiment was to determine the effect of having the middle robot occlude the acoustic signal between the first and third Maxelbots. The first follower (middle robot) tries to keep the leader at (0 cm, 63.5 cm) with respect to its local coordinate system. The second follower tries to keep the leader at (0 cm, 145 cm) with respect to its local coordinate system.

Table 3 summarizes the quality of the results. This first follower maintains position quite well. The second follower does exhibit some difficulties due to occlusion, since it does lag a bit behind the ideal distance. However, even in this case the distance is approximately only 10% off from the ideal distance. Also, the standard deviation is acceptably low.

Table 3. Accuracy of the two followers' X and Y positions in a linear formation (results in cm).

	Ideal	Mean	Std. dev.
Follower1-X	0	-1.5	0.8
Follower1-Y	63.5	67.1	1.0
Follower2-X	0	0.3	4.8
Follower2-Y	145	159.8	4.1

7.2 Accuracy of Non-Linear Formations

The second and third experiments examine the effect of position with respect to the quality of the results (trilateration accuracy can be affected by the difference in the bearing of one robot with respect to another [15]). We try two different configurations of the robots. In the first, there are three robots. The right follower tries to keep the leader at (-48 cm, 91 cm) with respect to its local coordinate system. The left follower tries to keep the leader at (53 cm, 91 cm) with respect to its local coordinate system. In the second configuration we use four Maxelbots in a diamond formation. In this latter experiment the wind speed near the ground ranged from 4 to 9 m/s.

Table 4 shows the XY-coordinates derived from the trilateration readings, for both configurations. From this table, it can be seen that the means are very close to the ideal.

Table 4. Accuracy of the followers' X and Y positions in a both formations (results in cm).

	Triangle			Diamond		
	Ideal	Mean	Std. dev.	Ideal	Mean	Std. dev
Follower1-X	-48	-53.0	3.3	61	62.2	1.8
Follower1-Y	91	97.8	2.8	61	54.9	2.8
Follower2-X	53	57.2	4.8	-61	-64.3	4.3
Follower2-Y	91	96.0	3.6	61	54.7	3.6
Follower3-X	-	-	-	0	1.0	5.1
Follower3-Y	-	-	-	122	111.8	4.6

The standard deviation is somewhat higher, reflecting the more difficult environmental conditions. However, very good formations are maintained by the trilateration system despite ground disturbances, wind, dust, and relatively high speed (Y has at most an error of roughly 11%). Results are averaged over five independent runs. Thus far no position-dependent effects have been noticed (other than distance, as is expected).

7.3 Trilateration Reliability Results

A detailed data analysis has been performed on the reliability of the trilateration system during the outdoor experiments. The RF failure rate is 0.2%. The rate at which the RF pulse is received but acoustic pings are not received (at all three receivers) is only 1%. Almost every acoustic failure was isolated, and not consecutive. Consider the interpretation of these results. Given that acoustic pings are sent at a rate of approximately four per second (4.17 Hz), this implies that 1% of the time, the Maxelbots ran for only 0.25 seconds on old data. Only once were two consecutive pings in a row not received, yielding one 0.5 second gap in readings.

Of all of our tests, the factor most important to success was the temperature. Below roughly 6°C the electronics failed. Given that our components are not ruggedized, this is not surprising.

8 Summary

This paper describes a 2D trilateration framework for the fast, accurate localization of neighboring robots. The framework uses three acoustic transducers and one RF transceiver. Our framework is designed to be modular, so that it can be used on different robotic platforms, and is not restricted to any particular class of control algorithms. Although we do not rely on GPS, stationary beacons, or environmental landmarks, their use is not precluded. Our framework is fully distributed, inexpensive, and scalable.

To illustrate the general utility of our framework, we demonstrated the application of our new robots in outdoor situations. The results from these experiments highlight the accuracy of our trilateration framework, as well as its current limitations (range and environmental temperature). For all of the Maxelbots, their X and Y positions are within roughly 11% of the desired values.

Open Source Project URL

The open source URL <http://www.cs.uwyo.edu/~wspears/maxelbot> provides schematic details and videos of this project. We thank the Joint Ground Robotics Enterprise for funding portions of this work.

References

1. Balch, T., Hybinette, M.: Social potentials for scalable multirobot formations. In: IEEE Transactions on Robotics and Automation. Volume 1. (2000) 73–80
2. Fax, J., Murray, R.: Information flow and cooperative control of vehicle formations. IEEE Transactions on Automatic Control **49** (2004) 1465–1476
3. Fierro, R., Song, P., Das, A., Kumar, V.: Cooperative control of robot formations. In Murphey, R., Pardalos, P., eds.: Cooperative Control and Optimization. Volume 66., Hingham, MA, Kluwer Academic Press (2002) 73–93
4. Brogan, D., Hodgins, J.: Group behaviors for systems with significant dynamics. Autonomous Robots **4** (1997) 137–153
5. Spears, W., Spears, D., Hamann, J., Heil, R.: Distributed, physics-based control of swarms of vehicles. Autonomous Robots **17**(2-3) (2004)
6. Borenstein, J., Everett, H., Feng, L.: Where am I? Sensors and Methods for Mobile Robot Positioning. University of Michigan (1996)
7. Thomas, F., Ros, L.: Revisiting trilateration for robot localization. IEEE Transactions on Robotics **21**(1) (2005) 93–101
8. Peasgood, M., Clark, C., McPhee, J. Localization of multiple robots with simple sensors. In: IEEE/RSJ International Conference on Intelligent Robots and Systems (IROS'05). (2005) 671–676
9. MacArthur, D.: Design and implementation of an ultrasonic position system for multiple vehicle control. Master's thesis, University of Florida (2003)
10. Nissanka, B., P.: The cricket indoor location system. Doctoral thesis, Massachusetts Institute of Technology, Cambridge, MA (2005)
11. Navarro-Serment, L., Paredis, C., Khosla, P.: A beacon system for the localization of distributed robotic teams. In: International Conference on Field and Service Robots, Pittsburgh, PA (1999) 232–237
12. Rothermich, J., Ecemis, I., Gaudiano, P.: Distributed localization and mapping with a robotic swarm. In Şahin, E., Spears, W., eds.: Swarm Robotics, Springer-Verlag (2004) 59–71
13. Payton, D., Estkowski, R., Howard, M.: Pheromone robotics and the logic of virtual pheromones. In Şahin, E., Spears, W., eds.: Swarm Robotics, Springer-Verlag (2004) 46–58
14. Spears, W., Hamann, J., Maxim, P., Kunkel, T., Heil, R., Zarzhitsky, D., Spears, D., Karlsson, C. Where are you? In Şahin, E., Spears, W., eds.: Swarm Robotics, Springer-Verlag (2006)
15. Heil, R.: A trilaterative localization system for small mobile robots in swarms. Master's thesis, University of Wyoming, Laramie, WY (2004)
16. Zarzhitsky, D., Spears, D., Spears, W.: Distributed robotics approach to chemical plume tracing. In: IEEE/RSJ International Conference on Intelligent Robots and Systems (IROS'05). (2005) 4034–4039
17. Hettiarachchi, S.: Distributed evolution for swarm robotics. Ph.D. thesis, University of Wyoming, Laramie, WY (2007)